PAPER

NJC
www.rsc.org/njc

Catalytic effect of Fe^{2+}, Cu^{2+} and UVA light on the electrochemical degradation of nitrobenzene using an oxygen-diffusion cathode

Enric Brillas,* Miguel Angel Baños, Sergi Camps, Conchita Arias, Pere-Lluís Cabot, José Antonio Garrido and Rosa María Rodríguez

Laboratori de Ciència i Tecnologia Electroquímica de Materials (LCTEM), Departament de Química Física, Facultat de Química, Universitat de Barcelona, Martí i Franquès 1-11, 08028, Barcelona, Spain. E-mail: brillas@ub.edu

Received (in Toulouse, France) 7th October 2003, Accepted 31st October 2003
First published as an Advance Article on the web 16th January 2004

The electrochemical treatment of 100 mg L^{-1} nitrobenzene solutions in 0.05 M Na_2SO_4 in the pH range 2.0–4.0 at 25 °C has been comparatively studied in the presence of Fe^{2+}, Cu^{2+} and/or UVA light as catalysts using an undivided cell with a Pt anode and an O_2-diffusion cathode able to electrogenerate H_2O_2. A quite slow degradation is found for the solution with 1 mM Cu^{2+} due to the low production of oxidizing hydroxyl radical ($OH^{\bullet}$) from anodic oxidation of water and the action of the Cu^{2+}/Cu^{+} system. Electro-Fenton treatment with 1 mM Fe^{2+} leads to a high concentration of $OH^{\bullet}$ in the medium from Fenton's reaction, but less than 70% of the nitrobenzene is mineralized since stable complexes of Fe^{3+} with products are formed. These complexes are quickly photodecomposed in the photoelectro-Fenton treatment of the same solution under UVA irradiation, leading to overall depollution at low currents. Complete degradation is also feasible using 1 mM Cu^{2+} and 1 mM Fe^{2+} at high current because $OH^{\bullet}$ can slowly destroy the complexes between Cu^{2+} and intermediates. The positive synergetic effect of all catalysts allows the quickest nitrobenzene mineralization using 1 mM Cu^{2+} and 1 mM Fe^{2+} under UVA irradiation. The nitrobenzene decay always follows a pseudo-first-order reaction. Aromatic products such as *o*-nitrophenol, *m*-nitrophenol, *p*-nitrophenol and 4-nitrocatechol have been followed by reverse-phase chromatography. Nitrate ions are formed from oxidation of nitroaromatic products. Generated carboxylic acids such as maleic, fumaric and oxalic have been detected by ion-exclusion chromatography. The different evolution of complexes of oxalic with Cu^{2+} and Fe^{3+} explains the influence of the catalysts on nitrobenzene degradation.

Introduction

Several indirect electro-oxidation treatments based on the combined use of cathodically generated hydrogen peroxide and iron ions as a catalyst have been recently developed for the degradation of toxic and biorefractory organic pollutants in acid waters.[1–20] In such methods, hydrogen peroxide is continuously supplied to the contaminated solution from the two-electron reduction of oxygen gas:

$$O_{2(g)} + 2H^+ + 2e^- \rightarrow H_2O_2 \qquad (1)$$

Reaction (1) can take place on graphite,[1] reticulated vitreous carbon,[2,3,8,11] mercury pool,[10,16] carbon felt[13,14,20] or O_2-diffusion[4,6,7,9,12,15,17–19] cathodes. Fe^{2+} is usually added to the acid solution to enhance the oxidizing power of H_2O_2, since Fe^{3+} and hydroxyl radical ($OH^{\bullet}$) are formed from the well-known classical Fenton reaction between Fe^{2+} and H_2O_2:[21–24]

$$Fe^{2+} + H_2O_2 \rightarrow Fe^{3+} + OH^{\bullet} + OH^- \qquad (2)$$

Hydroxyl radical thus produced is a non-selective and strong oxidant of organic pollutants, yielding dehydrogenated or hydroxylated derivatives that can be finally mineralized, that is converted into CO_2 and inorganic ions. In addition, $OH^{\bullet}$ can also rapidly react with Fe^{2+} to give Fe^{3+}:

$$Fe^{2+} + OH^{\bullet} \rightarrow Fe^{3+} + OH^- \qquad (3)$$

The second-order rate constant (k_2) for reaction (3) is 4.3×10^8 M^{-1} s^{-1},[22] a value several orders of magnitude higher than the 53 M^{-1} s^{-1} determined for reaction (2).[22] An advantage of the use of the Fe^{3+}/Fe^{2+} catalytic system is that Fe^{2+} is not removed from the solution by the above reactions, since it is continuously regenerated in small amounts from the reduction of Fe^{3+} with electrogenerated H_2O_2 by reaction (4) with $k_2 = 3.1 \times 10^{-3}$ M^{-1} s^{-1},[23] with hydroperoxyl radical ($HO_2^{\bullet}$) by reaction (5) with $k_2 < 1 \times 10^3$ M^{-1} s^{-1},[25] and/or with organic radical intermediates $R^{\bullet}$ by reaction (6).

$$Fe^{3+} + H_2O_2 \rightarrow Fe^{2+} + H^+ + HO_2^{\bullet} \qquad (4)$$

$$Fe^{3+} + HO_2^{\bullet} \rightarrow Fe^{2+} + H^+ + O_2 \qquad (5)$$

$$Fe^{3+} + R^{\bullet} \rightarrow Fe^{2+} + R^+ \qquad (6)$$

The existence of reactions (4)–(6) ensures the propagation of catalytic reaction (2) with the production of a sufficient concentration of $OH^{\bullet}$ in the medium for an efficient destruction of organic pollutants. The hydroperoxyl radical produced is a species with a much weaker oxidizing power than $OH^{\bullet}$.

The so-called electrogenerated Fenton's reagent (EFR)[1,8,10,11,13,14,20] is the most typical indirect electro-oxidation method with H_2O_2 electrogeneration. It consists of the treatment of an acid solution with a small concentration of Fe^{2+} or Fe^{3+} contained in the cathodic compartment of a divided electrolytic cell. When O_2 is bubbled through the solution, H_2O_2 is formed *via* reaction (1) and pollutants are destroyed by the $OH^{\bullet}$ produced in reaction (2). In previous work,[6,7,12,15,17–19] we have studied the degradative behavior of two other indirect electro-oxidation techniques, so-called electro-Fenton and photoelectro-Fenton, performed in an undivided cell with a Pt anode and a carbon–polytetrafluoroethylene (PTFE) O_2-fed cathode, which is able to produce H_2O_2 by reaction (1) at rates appropriate to the needs of

DOI: 10.1039/b312445b

effluent treatment. The electro-Fenton method involves the addition of catalytic Fe^{2+} to the initial acid solution to permit the main destruction of pollutants by $OH^{\bullet}$ generated in the medium by reaction (2), although they can also be degraded by reaction with adsorbed $OH^{\bullet}$ formed on the Pt anode surface from water oxidation:[26–29]

$$H_2O \rightarrow OH^{\bullet}_{ads} + H^+ + e^- \quad (7)$$

In the photoelectro-Fenton method, the solution is also irradiated with UVA light at $\lambda_{max} = 360$ nm to favor the regeneration of Fe^{2+} from additional photoreduction of $Fe(OH)^{2+}$, which is the predominant Fe^{3+} species at pH 3:[21,22]

$$Fe(OH)^{2+} + h\nu \rightarrow Fe^{2+} + OH^{\bullet} \quad (8)$$

Although reaction (8) accelerates the production of $OH^{\bullet}$ and hence, the mineralization of organics, the action of UVA light is much more complex, since it can photodecompose complexes of Fe^{3+} with some oxidation products, for example, oxalic acid.[30]

The above EFR, electro-Fenton and photoelectron-Fenton methods based on the use of iron ions as catalyst have been successfully utilized for the mineralization of aromatic compounds such as aniline,[4,7] phenol,[8,9] 4-chlorophenol,[6] chlorophenoxy herbicides,[10,12–15,17–19] atrazine[16] and bisphenol A.[20] However, less is known about other possible indirect electro-oxidation procedures involving $OH^{\bullet}$ production by Fenton-like reactions with catalysts different from iron ions. Recently, Gozmen *et al.*[20] reported that the EFR treatment of 200 mL of a 0.7 mM bisphenol A solution in 0.01 M HCl is more efficient than the analogous electrochemical degradation with electrogenerated H_2O_2 and Cu^{2+} as catalyst. In contrast, Gallard *et al.*[31] showed that the oxidation rate of a 1 μM atrazine solution of pH 3 by means of H_2O_2/Fe^{3+} is enhanced in the presence of Cu^{2+}, due to the generation of higher concentration of oxidizing $OH^{\bullet}$. To try to develop quicker oxidation methods for water remediation, more experimental effort is then needed to clarify the oxidative ability of indirect electro-oxidation systems containing Fe^{2+}, Cu^{2+} and UVA light as combined catalysts for H_2O_2 electrogeneration. In this way, we have undertaken a study to test the effects of such catalysts on the electrochemical destruction of nitrobenzene, a well-known toxic pollutant of industrial waste waters.[32] An efficient degradation of this compound in aqueous medium has been reported using some advanced oxidation processes (AOPs) in which the oxidizing agent $OH^{\bullet}$ is generated from chemical and photochemical systems such as H_2O_2/Fe^{2+},[33] H_2O_2/UV,[33,34] $H_2O_2/Fe^{3+}/UV$,[35] O_3,[36–39] O_3/H_2O_2,[32,37] O_3/UV,[32,37–39] $O_3/H_2O_2/UV$[37] and $O_3/Fe^{3+}/UV$.[38] Nitrophenols have been detected as primary products of nitrobenzene oxidation by O_3/H_2O_2 and O_3/UV.[32]

This paper reports the results obtained for the degradation of an acidic aqueous solution containing 100 mg L^{-1} of nitrobenzene and a low salt content of 0.05 M Na_2SO_4 of pH 3.0 in an undivided cell with a Pt anode and an O_2-diffusion cathode. Comparative electrolyses using 1 mM Cu^{2+}, 1 mM Fe^{2+} (electro-Fenton method), 1 mM Fe^{2+} + UVA light (photoelectro-Fenton method), 1 mM Cu^{2+} + 1 mM Fe^{2+} and 1 mM Cu^{2+} + 1 mM Fe^{2+} + UVA light as catalysts have been made at different currents to establish the oxidative ability of each system. The influence of pH and Cu^{2+} and Fe^{2+} concentrations upon the behavior of the combined methods has been studied. Stable products have been identified and quantified in each case and a reaction scheme for nitrobenzene mineralization involving all these species is proposed. The H_2O_2 accumulated in each electrolytic system without contaminants has been previously determined to clarify its catalytic effect.

Experimental

Chemicals

Nitrobenzene, *o*-nitrophenol, *m*-nitrophenol, *p*-nitrophenol, 4-nitrocatechol, maleic acid, fumaric acid and oxalic acid were reagent grade supplied by Merck and Fluka. Anhydrous sodium sulfate, used as background electrolyte, and heptahydrated ferrous sulfate and pentahydrated cupric sulfate, both used as catalysts, were analytical grade from Fluka. All acid solutions were prepared with high-purity water obtained from a Millipore Milli-Q system, with conductivity $< 6 \times 10^{-8}$ S cm^{-1} at 25 °C. The initial solution pH was adjusted with analytical grade sulfuric acid purchased from Merck. Organic solvents and the other chemicals employed were either HPLC or analytical grade from Merck, Fluka and Aldrich.

Instruments and analysis procedures

Electrochemical experiments were performed with an Amel 2049 potentiostat-galvanostat. The solution pH was measured with a Crison 2000 pH-meter. The concentration of H_2O_2 accumulated in the electrolyzed solutions at a given time was obtained from the light absorption of the colored titanic–hydrogen peroxide complex at $\lambda = 420$ nm,[40] determined with a Unicam UV4 Prisma double-beam spectrometer thermostatted at 25 °C. The mineralization of nitrobenzene solutions was monitored by the decay of their total organic carbon (TOC), obtained on a Shimadzu 5050 TOC analyzer using the standard non-purgeable organic carbon (NPOC) method. Before analysis, the samples extracted from electrolyzed solutions were filtered with 0.45 μm PTFE filters purchased from Whatman. The degradation of nitrobenzene and its aromatic intermediates was followed by reverse-phase chromatography with a Waters system. It consisted of a Waters 600 high performance liquid chromatograph (HPLC), fitted with a Spherisorb ODS2 5 μm, 150 × 4.6 mm, column at room temperature, and coupled with a Waters 996 photodiode array detector set at $\lambda = 280$ nm, controlled through a Millennium-32® program. Aliquots of 20 μL were injected into the HPLC chromatograph and a 50:45:5 (v/v/v) methanol–phosphate buffer (pH 2.5)–pentanol mixture was employed as eluent at 1.0 mL min^{-1}. Generated carboxylic acids were identified and quantified by ion-exclusion chromatography using the above HPLC chromatograph fitted with a Bio-Rad Aminex HPX 87H, 300 × 7.8 mm, column at 35 °C, along with the photodiode array detector set at $\lambda = 210$ nm. In this technique, samples of 20 μL were also analyzed and a 4 mM H_2SO_4 solution was employed as eluent at 0.6 mL min^{-1}. The concentration of nitrite and nitrate ions in the final electrolyzed solutions was determined by ion chromatography using a Kontron 600 HPLC, fitted with a Waters IC-Pak anion column at 35 °C and coupled with a Waters spectrophotometric detector. The eluent employed for ion chromatography was a borate–gluconate buffer of pH 8.5 and aliquots of 100 μL were injected into the liquid chromatograph after being ultramicrofiltrated by Ultrafree filters with a 10 000 Dalton cutoff. The concentration of iron ions and/or Cu^{2+} in solutions was obtained by inductively coupled plasma-atomic emission spectrometry (ICP-AES) using a Thermojarrell Ash Polyscan 61 E inductively coupled argon plasma spectroscope.

Electrolytic systems

All electrolyses were conducted in an open, undivided and thermostatted cylindrical cell containing a 100- mL solution stirred with a magnetic bar. The anode was a 10 cm^2 Pt sheet of 99.99% purity supplied by SEMPSA and the cathode was a 3.1 cm^2 carbon-PTFE electrode fed with pure O_2 at a rate of 20 mL min^{-1} to electrogenerate H_2O_2 from reaction (1). The

electrolytic setup and the preparation of the O_2-diffusion cathode have been described elsewhere.[4,12]

Solutions of 100 mL containing 100 mg L^{-1} of nitrobenzene (corresponding to 58.5 mg L^{-1} of TOC) in 0.05 M Na_2SO_4 adjusted to pH 2.0–4.0 using H_2SO_4 were comparatively degraded by the different treatments at constant currents (I) of 100, 300 and 450 mA. In all cases, the temperature was maintained at 25 °C. The catalytic influence of Cu^{2+} or Fe^{2+} was studied by adding 1 mM of each ion to the starting solution, while a concentration range 0.125–1 mM for both ions was used to test the combined effects of $Cu^{2+} + Fe^{2+}$. These ionic concentrations were chosen since 0.5–1 mM Fe^{2+} was found as optimal for the electro-Fenton and photoelectron-Fenton treatments of other aromatics in previous work.[12,15,17–19] The solutions were irradiated with a Philips 6 W fluorescent black light blue tube, which emitted UVA light in the wavelength region between 300 and 420 nm, with a maximum at $\lambda_{max} = 360$ nm. This tube was placed at the top of the open cell, 7 cm from the solution surface, supplying a photoionization energy input to the solution of 140 μW cm^{-2}, detected with a NRC 820 laser power meter working at 514 nm.

Results and discussion

Effect of catalysts on H_2O_2 accumulation

The ability of the system to accumulate the H_2O_2 produced by the O_2-diffusion cathode from reaction (1) was tested by electrolyzing 100 mL of a 0.05 M Na_2SO_4 solution of pH 3.0 at constant I for 6 h in the absence and presence of Cu^{2+}, Fe^{2+} and/or UVA light. As an example, Fig. 1 shows the evolution of H_2O_2 concentration at $I = 300$ mA under such conditions. In these experiments, a slow decay in solution pH with raising electrolysis time was observed, reaching a final pH value close to 2.6–2.8. In the absence of catalysts (curve a of Fig. 1), H_2O_2 is gradually accumulated in the solution during the first 3 h of electrolysis, where it attains a steady concentration close to 43 mM. In fact, a steady H_2O_2 concentration directly proportional to the applied current is found in the same solution when it is electrolyzed between 100 and 450 mA for long periods. This behavior can be explained by considering that the steady state involves electrogeneration and simultaneous destruction of H_2O_2 at the same rate, proportional to I. The disappearance of this species can then be related to its chemical and electrochemical decomposition to O_2 at the Pt anode.[4,12] The latter process can take place by the following reactions

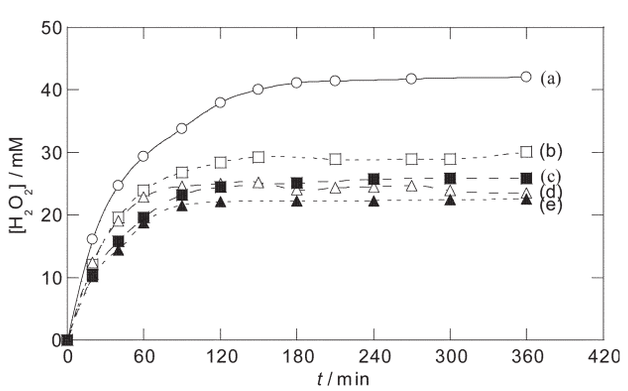

Fig. 1 Concentration of accumulated H_2O_2 *vs.* time during the electrolysis of 100 mL solutions of 0.05 M Na_2SO_4 of pH 3.0 in a cell containing a 10 cm^2 Pt anode and a 3.1 cm^2 O_2-diffusion cathode. (curve a, ○) Without catalyst. In the other cases, the solution contained the following catalysts: (curve b, □) 1 mM Fe^{2+} (electro-Fenton conditions); (curve c, ■) 1 mM Fe^{2+} + UVA light with $\lambda_{max} = 360$ nm (photoelectro-Fenton conditions); (curve d, △) 0.25 mM Cu^{2+} + 1 mM Fe^{2+}; (curve e, ▲) 0.25 mM Cu^{2+} + 1 mM Fe^{2+} + UVA light. Applied current 300 mA. Temperature 25 °C.

via $HO_2^{\bullet}$ formation:

$$H_2O_2 \rightarrow HO_2^{\bullet} + H^+ + e^- \quad (9)$$

$$HO_2^{\bullet} \rightarrow O_2 + H^+ + e^- \quad (10)$$

which compete with anodic oxidation of water to O_2 initiated by reaction (7).

Addition of 0.25 mM Cu^{2+} to the 0.05 M Na_2SO_4 solution of pH 3.0 caused a slow inhibition of H_2O_2 electrogeneration at all currents, because of the deposition of a reddish precipitate on the cathode surface that partially prevents reaction (1) and favors direct reduction of water to H_2 and OH^-. The formation rate of this precipitate increased with raising Cu^{2+} concentration up to 1 mM. The collected cathodic precipitate at the end of all electrolyses made with only Cu^{2+} was completely soluble in 1 M HNO_3, as expected if it is composed of $Cu(OH)_2$, a species which could be obtained by reaction of Cu^{2+} with OH^- present in high concentration near the cathode as product of reaction (1) and/or water reduction. However, no cathodic precipitate was detected when Fe^{2+} and/or organic contaminants were also present in the solution, probably due to the existence of other parallel reactions of Cu^{2+}, as will be discussed below. All these results allow us to conclude that reduction of Cu^{2+} to metallic Cu does not occur at the O_2-diffusion cathode.

By comparing curves a and b of Fig. 1, one can establish that less H_2O_2 is accumulated when 1 mM Fe^{2+} is added to the solution electrolyzed at 300 mA (electro-Fenton conditions). This trend can be ascribed to the higher decomposition rate of H_2O_2 by its homogeneous reaction with Fe^{2+} and Fe^{3+} from reactions (2) and (4), respectively. Under photoelectro-Fenton conditions at 300 mA (curve c of Fig. 1), a slightly higher decay in accumulated H_2O_2 is found, since UVA radiation enhances Fe^{2+} regeneration from reaction (8) giving rise to an increase in the rate of reactions (2)–(5). The presence of 0.25 mM Cu^{2+} + 1 mM Fe^{2+} as catalyst (curve d of Fig. 1) even favors a lower steady concentration of H_2O_2 than under electro-Fenton and photoelectro-Fenton conditions. This behavior can be associated with the participation of the Cu^{2+}/Cu^+ system in its decomposition to O_2. Thus, Cu^{2+} can react in the bulk solution with $HO_2^{\bullet}$ generated by reaction (4) to yield Cu^+ as follows:[31,41]

$$Cu^{2+} + HO_2^{\bullet} \rightarrow Cu^+ + H^+ + O_2 \quad (11)$$

Reaction (11) is very fast, with $k_2 = 5 \times 10^7$ M^{-1} s^{-1},[41] so that the resulting Cu^+ can quickly regenerate Cu^{2+} by oxidation either with H_2O_2 from reaction (12) with $k_2 = 1 \times 10^4$ M^{-1} s^{-1}[42] or with $OH^{\bullet}$ from reaction (13) with $k_2 = 1 \times 10^{10}$ M^{-1} s^{-1}:[43]

$$Cu^+ + H_2O_2 \rightarrow Cu^{2+} + OH^{\bullet} + OH^- \quad (12)$$

$$Cu^+ + OH^{\bullet} \rightarrow Cu^{2+} + OH^- \quad (13)$$

The faster disappearance of H_2O_2 in the presence of 0.25 mM Cu^{2+} and 1 mM Fe^{2+} than under electro-Fenton conditions (see curves b and d of Fig. 1) can then be due to the action of reactions (11)–(13) of the Cu^{2+}/Cu^+ system, running in parallel to reactions (2)–(5) of the Fe^{3+}/Fe^{2+} one. The slightly lower H_2O_2 accumulation shown in curve e of Fig. 1 at the same current using 0.25 mM Cu^{2+}, 1 mM Fe^{2+} and UVA light as catalysts can be ascribed to the additional regeneration of Fe^{2+} from reaction (8) that enhances reactions (2)–(5), destroying more H_2O_2. The fact that no cathodic precipitate of $Cu(OH)_2$ is formed when Fe^{2+} is also present in the solution could be related to the existence of the above catalytic loop for the Cu^{2+}/Cu^+ system, induced by that of the Fe^{3+}/Fe^{2+} one.

Comparative degradative behavior of nibrobenzene

The different indirect electro-oxidation treatments tested always led to a gradual depollution of all acidic 100 mg L^{-1}

nitrobenzene solutions with increasing electrolysis time. Reproducible values for TOC removal were obtained in all cases. Fig. 2 shows the comparative TOC abatement for the above solution at initial pH 3.0 when it is electrolyzed at 100 mA and at 25 °C for 6 h using 1 mM Cu^{2+} (curve a), 1 mM Fe^{2+} (curve b), 1 mM Cu^{2+} + 1 mM Fe^{2+} (curve c), 1 mM Fe^{2+} + UVA light (curve d) and 1 mM Cu^{2+} + 1 mM Fe^{2+} + UVA light (curve e). In these experiments, the solution pH remained practically constant, reaching a final value close to 2.8–2.9. A quite slow TOC decay can be observed in the presence of 1 mM Cu^{2+}, where only 53% mineralization is attained at the end of electrolysis. The very low oxidation ability of this method can be accounted for by the small $OH^{\bullet}$ concentration produced on the Pt anode surface from reaction (7),[12,15–19] which is the main oxidizing agent of nitrobenzene and its oxidation products. However, a much more complex degradative behavior of this electrolytic system is expected, since it is also possible that Cu^{2+} can form complexes with some intermediates (short organic diacids, for example) and/or can be reduced in the bulk solution with several radical organics $R^{\bullet}$:[31]

$$Cu^{2+} + R^{\bullet} \rightarrow Cu^{+} + R^{+} \qquad (14)$$

Note that the slow mineralization of contaminants shown in curve a of Fig. 2 suggests that Cu^{+} thus generated could only yield a small concentration of oxidizing $OH^{\bullet}$ from reaction (12). The existence of such competitive reactions for Cu^{2+} could also prevent the formation of a cathodic precipitate of $Cu(OH)_2$, only detected in the absence of organic pollutants, as stated above.

In contrast, in the presence of 1 mM Fe^{2+} (curve b of Fig. 2), the TOC of the nitrobenzene solution is rapidly reduced by 49% during the first 3 h of electrolysis, although if it is prolonged to 6 h, its degradation rate strongly falls to attain only 53% final TOC removal, a value similar to that obtained for the slower treatment with 1 mM Cu^{2+} at the same time (curve a of Fig. 2). The quick mineralization in the first 3 h of the electro-Fenton process can be related to the rapid homogeneous reaction of organics with the great amounts of $OH^{\bullet}$ produced from reaction (2), until the formation of difficulty oxidizable products, such as complexes of short organic diacids with Fe^{3+},[30] which are very slowly destroyed at longer times. A faster and gradual decay in TOC can be observed in curve c of Fig. 2 when the same solution is electrolyzed using 1 mM Cu^{2+} + 1 mM Fe^{2+}, attaining 88% mineralization at 6 h. This enhancement of the degradation process suggests the presence of other products that are more easily oxidized with $OH^{\bullet}$, mainly generated from Fenton's reaction (2) rather than from reactions (7) and (12). These species could be complexes of organic intermediates with Cu^{2+}, competitively formed with those of Fe^{3+}. The use of UVA light combined with 1 mM Fe^{2+} (curve d of Fig. 2) leads to complete mineralization of nitrobenzene (> 96% of TOC decay) at the end of electrolysis, although with a slightly slower degradation rate than for 1 mM Cu^{2+} + 1 mM Fe^{2+} + UVA light (curve e of Fig. 2). The overall TOC removal found under both conditions could be explained by the quick additional photodecomposition of stable products under electro-Fenton conditions and/or the enhancement of the generation rate of $OH^{\bullet}$ from reaction (8). The faster mineralization rate obtained by combining 1 mM Cu^{2+}, 1 mM Fe^{2+} and UVA light could then be associated with the existence of a parallel destruction of complexes of intermediates with Cu^{2+}.

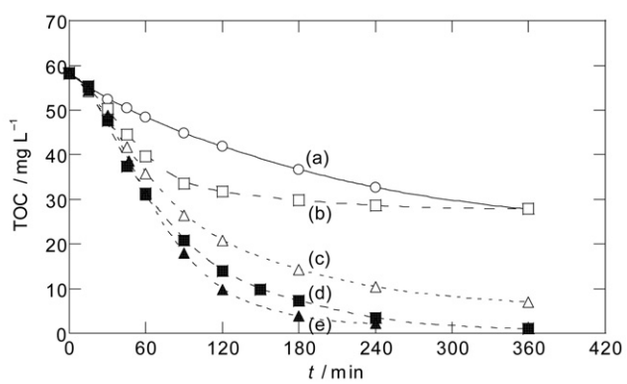

Fig. 2 TOC abatement with electrolysis time for the degradation of 100 mL of 100 mg L^{-1} nitrobenzene solutions in 0.05 M Na_2SO_4 of pH 3.0 at 100 mA and at 25 °C in a cell with a 10 cm^2 Pt anode and a 3.1 cm^2 O_2-diffusion cathode. Catalysts: (curve a, ○) 1 mM Cu^{2+}; (curve b, □) 1 mM Fe^{2+} (electro-Fenton process); (curve c, △) 1 mM Cu^{2+} + 1 mM Fe^{2+}; (curve d, ■) 1 mM Fe^{2+} + UVA light (photo-electro-Fenton process); (curve e, ▲) 1 mM Cu^{2+} + 1 mM Fe^{2+} + UVA light.

Apparent current efficiency

The electrochemical degradation of nitrobenzene in the presence of electrogenerated H_2O_2 depends on the catalyst tested, although in all cases its mineralization process involves the cleavage of the nitro group of nitro derivative intermediates during their oxidation with $OH^{\bullet}$. This has to lead to the release of nitrite and/or nitrate ions to the medium. To confirm this behavior, the amount of such ions present in the solutions with 1 mM Fe^{2+} + UVA light and 1 mM Cu^{2+} + 1 mM Fe^{2+} + UVA light after 6 h of electrolysis at 100 mA was quantified. While no nitrite ions were detected in both cases, NO_3^- concentrations of 48.5 and 49.9 mg L^{-1}, corresponding to a conversion of 96% and 99% of the initial nitro group into nitrate ion (50.4 mg L^{-1} for 100% conversion), were found in such mineralized solutions, respectively. These results allow us to conclude that only nitrate ion is produced during the electrochemical destruction of nitrobenzene. Consequently, its overall oxidation process involving its transformation into CO_2 and NO_3^- can be written as follows:

$$C_6H_5NO_2 + 13H_2O \rightarrow 6CO_2 + NO_3^- + 31H^+ + 31e^- \qquad (15)$$

which presupposes the consumption of 31 F per mole of compound.

From the above considerations, the apparent current efficiency (ACE) for each experiment was determined from the following expression:

$$ACE = [\Delta(TOC)_{expt}/\Delta(TOC)_{theor}] \times 100 \qquad (16)$$

where $\Delta(TOC)_{expt}$ is the experimental TOC decay in the solution at a given electrolysis time and $\Delta(TOC)_{theor}$ is the theoretically calculated TOC removal considering that the applied electrical charge (= current × time) is only consumed to mineralize nitrobenzene from reaction (15).

Fig. 3 shows the evolution of the efficiency calculated from eqn. (16) for the experiments given in Fig. 2. In the case of 1 mM Cu^{2+}, the system with the lowest oxidation ability, this parameter is low and always falls with raising electrolysis time from 13% at 15 min to 5.8% at 6 h. In contrast, all the other methods are much more efficient and their ACE increases during the first hour, reaching a maximum value of 21% for 1 mM Fe^{2+}, 26% for 1 mM Cu^{2+} + 1 mM Fe^{2+} and 31–32% for the two trials with UVA light. At longer times, the efficiency of these treatments is gradually reduced up to the end of electrolysis, so that at a given time a higher ACE value is found as the oxidation power of the electrolytic system increases in the sequence: 1 mM Fe^{2+} < 1 mM Cu^{2+} + 1 mM Fe^{2+} < 1 mM Fe^{2+} + UVA light ≤ 1 mM Cu^{2+} + 1 mM Fe^{2+} + UVA light (see Fig. 3). The increase in efficiency during the first hour of all these methods suggests a progressive formation of more

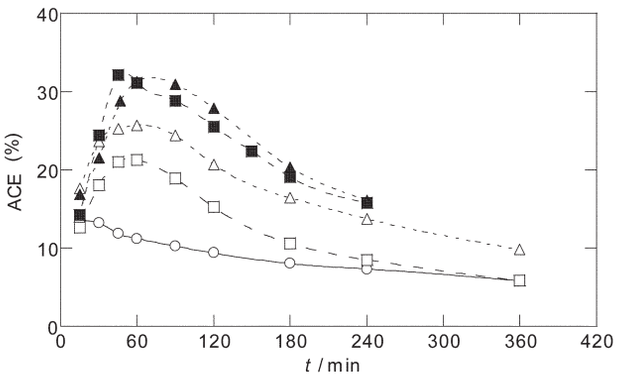

Fig. 3 Apparent current efficiency *vs.* electrolysis time for the experiments shown in Fig. 2.

easily oxidizable products than the initial nitrobenzene. The gradual decrease in ACE at longer times can then be accounted for by the progressive decay in pollutant concentration favoring the consumption of $OH^{\bullet}$ by other parallel non-oxidizing reactions. This change in the trend of efficiency does not occur when only 1 mM Cu^{2+} is used, since this catalyst produces a much smaller concentration of $OH^{\bullet}$ from reaction (12) than Fe^{2+} from reaction (2), yielding a slower degradation rate of all pollutants.

Influence of applied current, catalyst concentration and solution pH

The possible effect of applied current on the degradative behavior of each method was examined by electrolyzing the nitrobenzene solution of pH 3.0 at 100, 300 and 450 mA. The percentage of TOC removal and the corresponding ACE value found after 1 and 3 h of such experiments are listed in Table 1. In all cases, the solution TOC is more rapidly reduced with increasing *I*, indicating an enhancement of the degradation power of all electrolytic systems. This trend can be explained by the concomitant increase in the generation of adsorbed $OH^{\bullet}$ on the anode from reaction (7) and of H_2O_2 by the cathode from reaction (1), as pointed out above. The higher accumulation of H_2O_2 in the medium accelerates reactions (2) and (12), leading to a higher concentration of $OH^{\bullet}$, which favors the oxidation of pollutants. The results of Table 1 always show a poor mineralization using 1 mM Cu^{2+}, since a 51% TOC decay is only attained after 3 h at 450 mM. Under the same conditions, the use of 1 mM Fe^{2+} gives much more degradation, 69% TOC removal, because of the higher effectiveness of Fenton's reaction (2) than reaction (12) for $OH^{\bullet}$ production. In the presence of 1 mM Cu^{2+} + 1 mM Fe^{2+}, the solution TOC is rapidly reduced by 82% and 85% for 3 h at 300 and 450 mA, respectively. For both currents, more than 95% degradation was reached at 6 h, indicating that complete mineralization of nitrobenzene is feasible by this method if high currents are applied for long times. The same phenomenon takes place when the solutions with 1 mM Fe^{2+} and 1 mM Cu^{2+} + 1 mM Fe^{2+} are irradiated with UVA light, although lower times are required for total mineralization, decreasing with increasing *I*. For example, the time needed to destroy 96% of pollutants using 1 mM Cu^{2+} + 1 mM Fe^{2+} + UVA light is reduced from 4 h at 100 mA (see curve e of Fig. 2) to 3 h at 450 mA (see Table 1). On the other hand, a gradual decrease in ACE with raising *I* can be observed in Table 1 at each time of all methods tested, suggesting that the gradual higher concentration of $OH^{\bullet}$ produced on the anode and in the medium accelerates its non-oxidizing reactions, such as its recombination into H_2O_2.

In previous work[12,15–19] we have reported that a catalytic Fe^{2+} concentration of 0.5–1 mM is enough to efficiently destroy aromatics at pH 3.0 in the electro-Fenton and photoelectro-Fenton methods. To verify if this behavior can be extended to the use of Cu^{2+} combined with Fe^{2+}, several 100 mg L^{-1} nitrobenzene solutions of pH 3.0 containing different concentrations of both ions between 0.125 and 1 mM were electrolyzed at 100 mA. The comparative TOC removal for these experiments without UVA irradiation is depicted in Fig. 4. As can be seen, a similar TOC decay is found in all cases, leading to about 88–91% mineralization at 6 h, except for 0.25 mM Cu^{2+} + 1 mM Fe^{2+} where the solution TOC is only reduced by 82% due to a slightly slower degradation rate of pollutants. When the same solutions were treated under UVA irradiation, similar TOC *vs.* time plots to those shown in curve e of Fig. 2 were also obtained. ICP-AES analysis of the initial solution with 1 mM Cu^{2+} + 1 mM Fe^{2+} and solutions collected after 6 h of electrolysis at 100 mA with and without UVA irradiation revealed that the concentration of iron ions (Fe^{2+} and Fe^{3+}) and Cu^{2+} does not vary with time, confirming that such ions are not deposited on the O_2-diffusion cathode. One can then conclude that optimum Cu^{2+} and Fe^{2+}

Table 1 Percentage of TOC removal and apparent current efficiency (ACE) for the mineralization of 100 mL of 100 mg L^{-1} nitrobenzene solutions in 0.05 M Na_2SO_4 of pH 3.0 at several currents and at 25 °C using different catalysts. Electrolyses were carried out in a one-compartment cell with a 10 cm^2 Pt anode and a 3.1 cm^2 O_2-diffusion cathode for H_2O_2 electrogeneration

		After 1 h of treatment		After 3 h of treatment	
Catalyst	*I*/mA	% TOC removal	ACE	% TOC removal	ACE
1 mM Cu^{2+}	100	17	11	37	8.3
	300	20	4.5	42	3.2
	450	25	3.7	51	2.5
1 mM Fe^{2+} [a]	100	31	21	49	11
	300	50	11	65	4.9
	450	52	7.8	69	3.4
1 mM Fe^{2+} + 1 mM Cu^{2+}	100	39	26	75	17
	300	61	14	82	6.2
	450	64	9.6	85	4.2
1 mM Fe^{2+} + UVA light [b]	100	46	31	87	20
	300	64	15	91	6.9
	450	66	9.9	93	4.6
1 mM Fe^{2+} + 1 mM Cu^{2+} + UVA light	100	47	32	93	21
	300	72	17	95	7.1
	450	73	11	96	4.8

[a] Electro-Fenton process. [b] Photoelectron-Fenton process using 6 W UVA light at λ_{max} = 360 nm for solution irradiation.

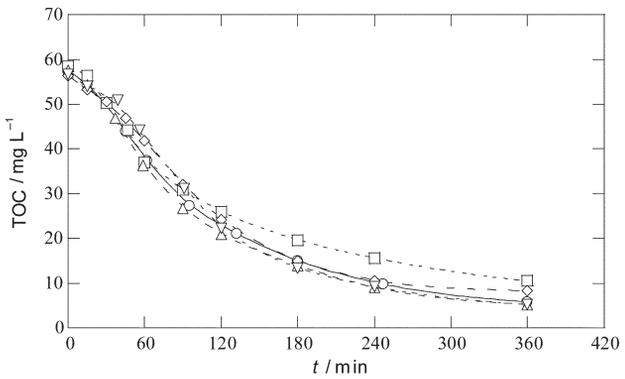

Fig. 4 Variation of TOC removal with electrolysis time for the treatment of 100 mL of 100 mg L^{-1} nitrobenzene solutions with different Fe^{2+} and Cu^{2+} concentrations as catalysts in 0.05 M Na_2SO_4 of pH 3.0 at 100 mA and at 25 °C using a cell containing a 10 cm^2 Pt anode and a 3.1 cm^2 O_2-diffusion cathode. (○) 1 mM Cu^{2+} + 1 mM Fe^{2+}; (□) 0.25 mM Cu^{2+} + 1 mM Fe^{2+}; (△) 0.5 mM Cu^{2+} + 0.5 mM Fe^{2+}; (◇) 1 mM Cu^{2+} + 0.25 mM Fe^{2+}; (▽) 1 mM Cu^{2+} + 0.125 mM Fe^{2+}.

concentrations between 0.5 and 1 mM can be utilized for an efficient destruction of nitrobenzene by electrochemical methods with H_2O_2 electrogeneration combining both ions as catalysts in the presence and absence of UVA light.

A more significant degradative effect was found when the initial pH of the nitrobenzene solution was varied between 2.0 and 4.0 using 1 mM Fe^{2+}, 1 mM Fe^{2+} + UVA light, 1 mM Cu^{2+} + 1 mM Fe^{2+} and 1 mM Cu^{2+} + 1 mM Fe^{2+} + UVA light. Electrolyses of all these solutions at 100 mA always yielded the quickest TOC removal at pH 3.0, although at pH 2.0 and 4.0 good degradation rates were also obtained. As an example, Fig. 5 shows this behavior for 1 mM Cu^{2+} + 1 mM Fe^{2+}, where at 6 h a 88% TOC decay takes place at pH 3.0, decreasing to 74% at pH 2.0 and 78% at pH 4.0. The final pH of such treated solutions was 2.8, 2.0 and 3.3, respectively. From these results, one can establish that pH 3.0 is optimal for methods involving at least Fe^{2+} as the catalyst. This can be related to the production ability of the main oxidizing agent $OH^•$ from reaction (2). Since the optimum pH for this reaction is 2.8,[21,22] it can be expected that the highest generation rate of $OH^•$ in the medium occurs at pH 3.0, yielding the fastest destruction of pollutants.

Nitrobenzene decay and evolution of intermediates

The destruction of nitrobenzene by reaction with the oxidants (mainly $OH^•$) generated in the treatments carried out on solutions of pH 3.0 at 100 mA was followed by reverse-phase chromatography, where it displayed a well-defined peak with a retention time (t_r) of 3.60 min. The change of its concentration with electrolysis time is presented in Fig. 6(a) for 1 mM Cu^{2+} and in Fig. 6(b) for the other catalysts. When only the Cu^{2+}/Cu^+ system is used, nitrobenzene undergoes a very slow decay up to its practicalyl complete disappearance from the medium in 6 h, in agreement with its slow TOC removal (see curve a of Fig. 2) due to the small $OH^•$ concentration produced by reactions (7) and (12). In contrast, Fig. 6(b) shows a quite fast destruction of this compound in 25–35 min with a similar rate for all the other treatments, involving at least the Fe^{3+}/Fe^{2+} catalytic system, thus confirming that it is mainly destroyed by the large amounts of $OH^•$ generated from Fenton's reaction (2). These results also indicate that nitrobenzene is not directly photolyzed under the experimental conditions tested.

The above nitrobenzene concentration decays were analyzed from kinetic equations related to different reaction orders and only good linear plots, with regression coefficients > 0.995, were found when they were fitted to a pseudo-first-order reaction at electrolysis times up to 25–30 min. This kinetic analysis is shown in the insets of Figs. 6(a) and 6(b). A pseudo-first-order rate constant (k) of 8.5×10^{-3} min^{-1} is thus obtained for 1 mM Cu^{2+}, a value much lower than the 0.115 min^{-1} for 1 mM Fe^{2+}, 0.136 min^{-1} for 1 mM Fe^{2+} + UVA light, 0.146 min^{-1} for 1 mM Cu^{2+} + 1 mM Fe^{2+} and 0.163 min^{-1} for 1 mM Cu^{2+} + 1 mM Fe^{2+} + UVA light. This behavior suggests the existence of a practically constant concentration of $OH^•$ in solution during all treatments. The slight increase in k value for 1 mM Fe^{2+} + UVA light than under similar electro-Fenton conditions can be accounted for by the continuous regeneration of Fe^{2+} from reaction (8), which increases the

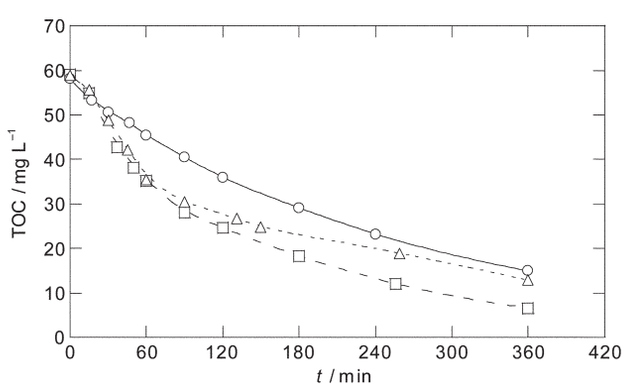

Fig. 5 Effect of pH on TOC decay of 100 mL solutions containing 100 mg L^{-1} nitrobenzene and 1 mM Cu^{2+} + 1 mM Fe^{2+} as catalysts at 100 mA and at 25 °C using a cell with a 10 cm^2 Pt anode and a 3.1 cm^2 O_2-diffusion cathode. Initial solution pH: (○) 2.0; (□) 3.0; (△) 4.0.

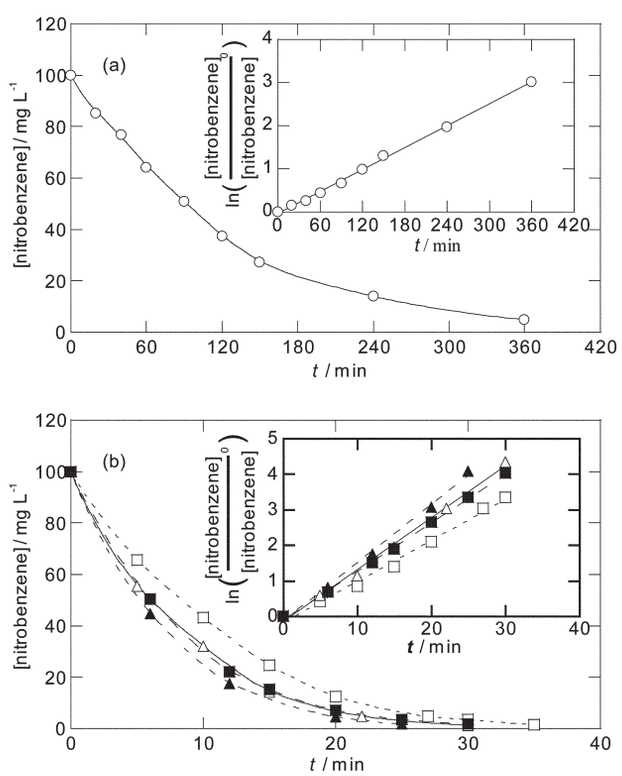

Fig. 6 Nitrobenzene concentration decay with electrolysis time during the degradation of 100 mL of 100 mg L^{-1} nitrobenzene solutions under the same conditions as Fig. 2. In plot a, the catalyst is 1 mM Cu^{2+}. In plot b, catalysts are: (□) 1 mM Fe^{2+}; (△) 1 mM Cu^{2+} + 1 mM Fe^{2+}; (■) 1 mM Fe^{2+} + UVA light; (▲) 1 mM Cu^{2+} + 1 mM Fe^{2+} + UVA light. The inset in each plot represents the corresponding kinetic analysis related to a pseudo-first-order reaction for nitrobenzene.

rate of Fenton's reaction (2) to yield a slightly higher steady concentration of $OH^{\bullet}$ that accelerates nitrobenzene destruction. However, this process seems less efficient to produce oxidizing $OH^{\bullet}$ than that of reactions (11)–(14) of the Cu^{2+}/Cu^{+} system, since the k value for 1 mM Cu^{2+} + 1 mM Fe^{2+} is even higher than that of 1 mM Fe^{2+} + UVA light. The positive synergetic effect of all these reaction explains the highest k value found when Cu^{2+}, Fe^{2+} and UVA light are simultaneously combined.

Reverse-phase chromatography was also utilized to analyze the aromatic intermediates formed during the degradation of the same nitrobenzene solutions. In all cases, the recorded chromatograms showed peaks related to monohydroxylated derivatives such as *p*-nitrophenol at $t_r = 2.46$ min, *m*-nitrophenol at $t_r = 3.13$ min and *o*-nitrophenol at $t_r = 3.41$ min, and the dihydroxylated 4-nitrocatechol at $t_r = 2.60$ min. These nitroaromatics were unequivocally identified by comparing their retention times and UV-Vis spectra, measured on the photodiode array, with those of pure products.

The evolution of such aromatic intermediates was followed by determining their concentrations as a function of electrolysis time by calibration with pure compounds. Fig. 7(a) shows that *o*-nitrophenol is the main nitroaromatic accumulated in the medium using 1 mM Cu^{2+}, with a maximum concentration of about 18 mg L^{-1} between 90 and 180 min, rapidly falling to less than 4 mg L^{-1} at 6 h. The same trend can be observed for 4-nitrocatechol, *m*-nitrophenol and *p*-nitrophenol, with maximum accumulations of 6.6, 5.2 and 1.2 mg L^{-1} around 150 min, respectively. The small proportion of the two latter nitrophenols in relation to *o*-nitrophenol can be ascribed to their fast hydroxylation with $OH^{\bullet}$ to give 4-nitrocatechol. A similar product distribution with electrolysis time is found using the other four treatments, although all nitroaromatics are rapidly destroyed in less than 35 min, as can be seen in Fig. 7(b) for 1 mM Cu^{2+} + 1 mM Fe^{2+} with and without UVA irradiation. This figure also shows the weak effect of UVA light on the time course of all products, thus discounting their direct photodecomposition. Comparison of Figs. 7(a) and 7(b) with Figs. 6(a) and 6(b) allows the conclusion that all nitroaromatic intermediates are only present in the medium while nitrobenzene is being decomposed, and hence, their destruction can not explain the change in TOC decay found for the different catalytic systems tested (see Fig. 2). To try to clarify this point, the evolution of generated carboxylic acids, expected from the oxidative cleavage of the benzenic ring of aromatic intermediates,[12,15–22] was studied.

Ion-exclusion chromatograms of the same electrolyzed solutions exhibited peaks associated with carboxylic acids such as oxalic at $t_r = 6.74$ min, maleic at $t_r = 8.24$ min and fumaric at $t_r = 15.7$ min. In all cases, maleic and fumaric acids only appear in the medium with concentrations lower than 1.5 mg L^{-1} for times shorter than 2 h. This indicates a rapid oxidation of both products with $OH^{\bullet}$ to oxalic acid.[15,21,22] A very different behavior can be seen in Fig. 8 for this acid, since its evolution depends on the catalyst used. For the Cu^{2+}/Cu^{+} system, it is slowly accumulated to about 35 mg L^{-1} at 150 min, while at longer times its concentration gradually decreases to *ca.* 10 mg L^{-1} at 6 h. The same trend can be observed using 1 mM Cu^{2+} + 1 mM Fe^{2+}, where oxalic acid attains a maximum concentration of about 57 mg L^{-1} at 1 h that drops to *ca.* 21 mg L^{-1} at 6 h. In contrast, this acid is continuously accumulated for 2 h by electro-Fenton to attain a steady concentration close to 73 mg L^{-1}, but it is completely mineralized by photoelectro-Fenton and 1 mM Cu^{2+} + 1 mM Fe^{2+} + UVA light at 3 h after reaching maximum accumulations of 60 and 37 mg L^{-1} at 50 min, respectively (see Fig. 8). In fact, the latter method yields the fastest destruction of oxalic acid, in agreement with the quickest TOC removal found for nitrobenzene (see curve e of Fig. 2).

Zuo and Hoigné[30] reported that oxalic acid forms stable complexes with Fe^{3+}, which can be photodecarboxylated by UVA light. Consequently, a large proportion of Fe^{3+}–oxalate complexes can be expected in the electrolyzed nitrobenzene solution using 1 mM Fe^{2+} at pH 3.0, due to the efficient generation of Fe^{3+} from reaction (2). Fig. 8 shows that these complexes cannot be mineralized under these conditions, where large amounts of $OH^{\bullet}$ are produced by reaction (2), limiting the oxidative ability of the electro-Fenton process. The steady concentration of near 73 mg L^{-1} of oxalic acid reached after 2 h of this treatment corresponds to about 19 mg L^{-1} of TOC, that is 70% of the final TOC value attained by the 100 mg L^{-1} nitrobenzene solution during electrolysis at 100 mA (see

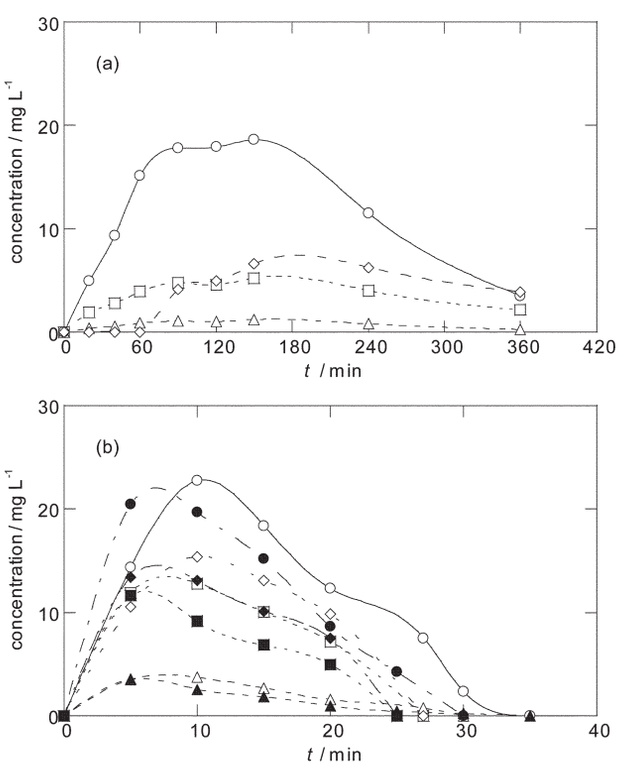

Fig. 7 Time-course of the concentration of aromatic intermediates: (○, ●) *o*-nitrophenol; (□, ■) *m*-nitrophenol; (△, ▲) *p*-nitrophenol; (◇,◆) 4-nitrocatechol during the degradation of 100 mg L^{-1} nitrobenzene solutions under the conditions given in Fig. 2. In plot a, the catalyst is 1 mM Cu^{2+}. In plot b, catalysts are: (○,□,△,◇) 1 mM Cu^{2+} + 1 mM Fe^{2+}; (●,■,▲,◆) 1 mM Cu^{2+} + 1 mM Fe^{2+} + UVA light.

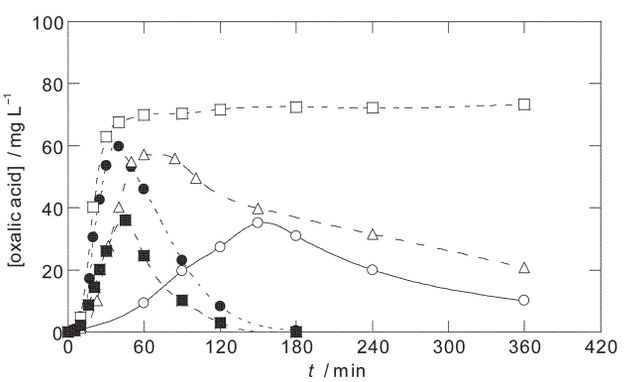

Fig. 8 Evolution of oxalic acid concentration during the treatment of 100 mg L^{-1} nitrobenzene solutions under the same conditions as in Fig. 2. Catalysts: (○) 1 mM Cu^{2+}; (□) 1 mM Fe^{2+}; (△) 1 mM Cu^{2+} + 1 mM Fe^{2+}; (●) 1 mM Fe^{2+} + UVA light; (■) 1 mM Cu^{2+} + 1 mM Fe^{2+} + UVA light.

curve b of Fig. 2). This indicates that other difficultly oxidizable products with $OH^{\bullet}$, different from Fe^{3+}–oxalato complexes, also exist in the final solution degraded by electro-Fenton, probably involving complexes of Fe^{3+} with other intermediates (diols, diacids, *etc.*). The efficient destruction of all these complexes under the action of UVA light can account for the fast and complete mineralization of nitrobenzene by photoelectro-Fenton. On the other hand, when only the Cu^{2+}/Cu^{+} system is used, a large proportion of Cu^{2+}–oxalato complexes are expected to be present in the medium, which are slowly destroyed with $OH^{\bullet}$ generated from reactions (7) and (12), as can be seen in Fig. 8. In the presence of 1 mM Cu^{2+} + 1 mM Fe^{2+}, both Cu^{2+}–oxalato and Fe^{3+}–oxalato complexes are produced, but only the complexes of Cu^{2+} can be mineralized by $OH^{\bullet}$, mainly generated from reaction (2). This causes a continuous shift of their equilibria towards the formation of more Cu^{2+}–oxalato complexes, leading to a slow and continuous TOC removal of the electrolyzed solution (see curve c of Fig. 2) and overall depollution at high currents. The quickest mineralization of nitrobenzene using 1 mM Cu^{2+} + 1 mM Fe^{2+} + UVA light can thus be related to the oxidation of Cu^{2+}–oxalato complexes with $OH^{\bullet}$ in parallel to the photodecomposition of complexes of Fe^{3+} by UVA light.

Proposed reaction sequence

A general pathway for the mineralization of nitrobenzene in acid media with electrogenerated H_2O_2 and Fe^{2+}, Cu^{2+} and/or UVA light as catalysts is proposed in Fig. 9. The sequence involves all intermediates detected, only showing the main oxidizing agent $OH^{\bullet}$ for sake of simplicity, although parallel reactions with other oxidants (H_2O_2, $HO_2^{\bullet}$, Cu^{2+}, *etc.*) are also possible. The process is initiated by $OH^{\bullet}$ attack on the C(2), C(3) and C(4) positions of nitrobenzene yielding *o*-nitrophenol, *m*-nitrophenol and *p*-nitrophenol, respectively, as the primary oxidation products. Further hydroxylation of the two latter nitrophenols gives 4-nitrocatechol. Probably *o*-nitrophenol is also hydroxylated, but the resulting diol is not accumulated in the medium. Parallel degradation of 4-nitrocatechol and other possible diols, with loss of a nitrate ion, leads to a mixture of maleic and fumaric acids, which are subsequently oxidized to oxalic acid. This acid is slowly converted into CO_2 by $OH^{\bullet}$, since it mainly forms complexes with Cu^{2+} and/or Fe^{3+} when one or both catalysts are present in the medium. While Cu^{2+}–oxalato complexes can be mineralized with $OH^{\bullet}$, Fe^{3+}–oxalato complexes are very stable under electro-Fenton conditions, although they can be quickly photodecarboxylated with loss of Fe^{2+} under the action of UVA light, as proposed by Zuo and Hoigné.[30]

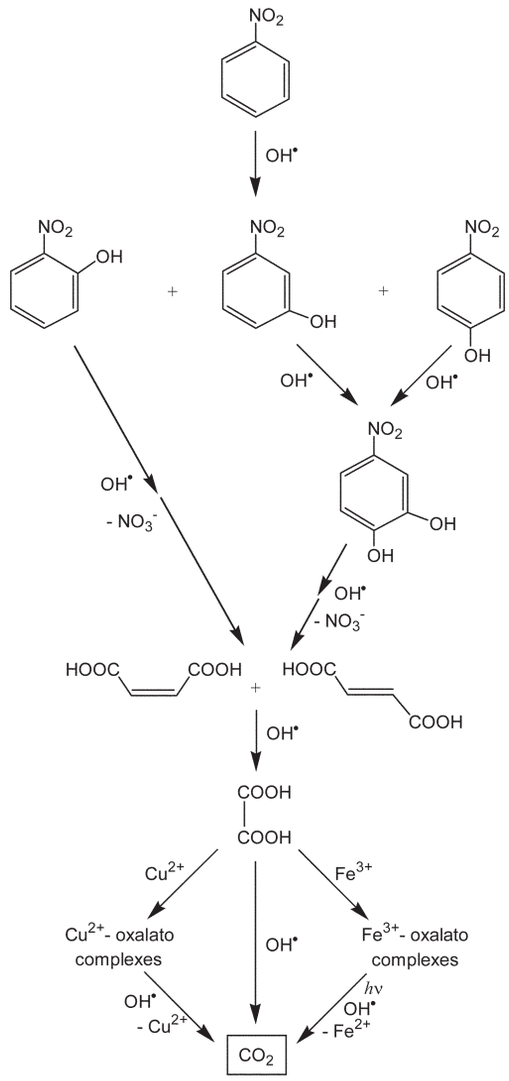

Fig. 9 Proposed reaction sequence for the electrochemical degradation of nitrobenzene at pH 3.0 in the presence of electrogenerated H_2O_2 with Fe^{2+}, Cu^{2+} and/or UVA light as catalysts.

Conclusions

The combined use of 1 mM Fe^{2+}, 1 mM Cu^{2+} and UVA light as catalysts allows a fast and complete degradation of acidic aqueous solutions of 100 mg L^{-1} of nitrobenzene at low current using a Pt anode and an O_2-diffusion cathode able to electrogenerate H_2O_2. This behavior is made feasible by the high concentration of oxidizing $OH^{\bullet}$ produced from Fenton's reaction, which can destroy complexes of Cu^{2+} with intermediates, along with the parallel photolysis of complexes formed with Fe^{3+}. This treatment is slightly more efficient than the photoelectro-Fenton one with 1 mM Fe^{2+} and UVA irradiation, indicating the existence of a positive synergetic effect of the Cu^{2+}/Cu^{+} and Fe^{3+}/Fe^{2+} catalytic systems. This also explains the overall mineralization of the same solution with 1 mM Fe^{2+} and 1 mM Cu^{2+} at high currents for long periods. When the electro-Fenton method is applied under comparable conditions, less than 70% degradation is reached due to the formation of hardly oxidizable products with $OH^{\bullet}$. The optimum operative conditions for all these electrolytic systems are attained when working with 0.5–1 mM of Fe^{2+} and/or Cu^{2+} at pH 3.0. In contrast, the use of only 1 mM Cu^{2+} leads to a very slow destruction of pollutants, since a low concentration of $OH^{\bullet}$ is obtained from water oxidation at the Pt anode and reaction of Cu^{+} with electrogenerated H_2O_2. Nitrobenzene decay always follows a pseudo-first-order reaction, with higher rate as the treatment becomes more oxidant. Its nitro group is initially released to the medium in the form of nitrate ion. In all cases, *o*-nitrophenol, *m*-nitrophenol, *p*-nitrophenol and 4-nitrocatechol have been identified and quantified as aromatic products by reverse-phase chromatography. Ion-exclusion chromatograms of the same electrolyzed solutions reveal the generation of maleic and fumaric acids from the oxidation of such intermediates. Both carboxylic acids are rapidly converted into oxalic acid, which can form Cu^{2+}–oxalato and Fe^{3+}–oxalato complexes when electrolysis is carried out in the presence of Cu^{2+} and/or Fe^{2+}, respectively. Fe^{3+}–oxalato complexes remain in the solution under electro-Fenton conditions, being rapidly photodecarboxylated by UVA light. The slow mineralization of Cu^{2+}–oxalato complexes with $OH^{\bullet}$ can account for the complete depollution of the solution with 1 mM Cu^{2+} and 1 mM Fe^{2+} and the highest oxidation ability of the catalytic system with Fe^{2+}, Cu^{2+} and UVA light.

Acknowledgements

The authors wish to give thanks for the financial support of MCYT (Ministerio de Ciencia y Tecnología, Spain) under project BQU2001-3712.

References

1 J. S. Do and C. P. Chen, *J. Electrochem. Soc.*, 1993, **140**, 1632.
2 Y. L. Hsiao and K. Nobe, *J. Appl. Electrochem.*, 1993, **23**, 943.
3 C. Ponce de Leon and D. Pletcher, *J. Appl. Electrochem.*, 1995, **25**, 307.
4 E. Brillas, E. Mur and J. Casado, *J. Electrochem. Soc.*, 1996, **143**, L49.
5 K. Rajeshwar and J. Ibañez, *Environmental Electrochemistry. Fundamentals and Applications in Pollution Abatement*, Academic Press, San Diego, 1997, ch. 5.
6 E. Brillas, R. Sauleda and J. Casado, *J. Electrochem. Soc.*, 1997, **144**, 2374.
7 E. Brillas, E. Mur, R. Sauleda, L. Sánchez, J. Peral, X. Domènech and J. Casado, *Appl. Catal., B*, 1998, **16**, 31.
8 A. Alvarez-Gallegos and D. Pletcher, *Electrochim. Acta*, 1999, **44**, 2483.
9 T. Harrington and D. Pletcher, *J. Electrochem. Soc.*, 1999, **146**, 2983.
10 M. A. Oturan, J. J. Aaron, N. Oturan and J. Pinson, *Pestic. Sci.*, 1999, **55**, 558.
11 D. Pletcher, *Acta Chem. Scand.*, 1999, **53**, 745.
12 E. Brillas, J. C. Calpe and J. Casado, *Water Res.*, 2000, **34**, 2253.
13 M. A. Oturan, *J. Appl. Electrochem.*, 2000, **30**, 475.
14 J. J. Aaron and M. A. Oturan, *Turk. J. Chem.*, 2001, **25**, 509.
15 B. Boye, M. M. Dieng and E. Brillas, *Environ. Sci. Technol.*, 2002, **36**, 3030.
16 A. Ventura, G. Jacquet, A. Bermond and V. Camel, *Water Res.*, 2002, **36**, 3517.
17 E. Brillas, B. Boye and M. M. Dieng, *J. Electrochem. Soc.*, 2003, **150**, E148.
18 B. Boye, E. Brillas and M. M. Dieng, *J. Electroanal. Chem.*, 2003, **540**, 25.
19 B. Boye, M. M. Dieng and E. Brillas, *Electrochim. Acta*, 2003, **48**, 781.
20 B. Gozmen, M. A. Oturan, N. Oturan and O. Erbatur, *Environ. Sci. Technol.*, 2003, **37**, 3716.
21 J. J. Pignatello, *Environ. Sci. Technol.*, 1992, **26**, 944.
22 Y. Sun and J. J. Pignatello, *Environ. Sci. Technol.*, 1993, **27**, 304.
23 J. De Laat and H. Gallard, *Environ. Sci. Technol.*, 1999, **33**, 2726.
24 G. F. Ijpelaar, M. Groenendijk, J. C. Kruitof and J. C. Schippers, *Water Sci. Technol.: Water Supply*, 2002, **2**, 229.
25 J. D. Rush and B. H. J. Bielski, *J. Phys. Chem.*, 1985, **89**, 5062.
26 C. Comninellis and A. De Battisti, *J. Chim. Phys.*, 1996, **93**, 673.
27 N. B. Tahar and A. Savall, *J. Electrochem. Soc.*, 1998, **145**, 3427.
28 F. Bonfatti, S. Ferro, F. Lavezzo, M. Malacarne, G. Lodi and A. De Battisti, *J. Electrochem. Soc.*, 2000, **147**, 592.
29 J. Iniesta, P. A. Michaud, M. Panizza, G. Cerisola, A. Aldaz and C. Comninellis, *Electrochim. Acta*, 2001, **46**, 3573.
30 Y. Zuo and J. Hoigné, *Environ. Sci. Technol.*, 1992, **26**, 1014.
31 H. Gallard, J. de Laat and B. Legube, *Rev. Sci. Eau*, 1999, **12**, 713.
32 F. J. Beltrán, J. M. Encinar and M. A. Alonso, *Ind. Eng. Chem. Res.*, 1998, **37**, 32.
33 E. Lipczynska-Kochany, *Chemosphere*, 1992, **24**, 1369.
34 F. S. García-Einschlag, J. López, L. Carlos, A. L. Capparelli, A. M. Braun and E. Oliveros, *Environ. Sci. Technol.*, 2002, **36**, 3936.
35 M. Rodríguez, A. Kirchner, S. Contreras, E. Chamarro and S. Esplugas, *J. Photochem. Photobiol, A*, 2000, **133**, 123.
36 F. J. Beltrán, J. M. Encinar and M. A. Alonso, *Ind. Eng. Chem. Res.*, 1998, **37**, 25.
37 F. J. Beltrán, J. Ribas, P. M. Álvarez, M. A. Alonso and B. Acedo, *Ind. Eng. Chem. Res.*, 1999, **38**, 4189.
38 S. Contreras, M. Rodríguez, E. Chamarro and S. Esplugas, *J. Photochem. Photobiol. A*, 2001, **142**, 79.
39 A. Latifoglu and D. M. Gurol, *Water Res.*, 2003, **37**, 1879.
40 *Standard Methods of Chemical Analysis*, 6th edn., ed. F. J. Welcher, R.E. Krieger Pub. Co., Huntington, NY, 1975, vol. 2, Part B, pp. 1827–1828.
41 B. H. J. Bielski, D. E. Cabelli, R. L. Arudi and A. B. Ross, *J. Phys. Chem. Ref. Data*, 1985, **14**, 1041.
42 V. K. Sharma and F. J. Millero, *Environ. Sci. Technol.*, 1988, **22**, 768.
43 G. U. Buxton, C. L. Greenstock, W. P. Helman and A. B. Ross, *J. Phys. Chem. Ref. Data*, 1988, **17**, 513.